

# Rhythm of Opinion: A Hawkes-Graph Framework for Dynamic Propagation Analysis

Yulong Li<sup>1,2\*</sup>, Zhixiang Lu<sup>1\*</sup>, Feilong Tang<sup>2,3</sup>, Simin Lai<sup>2,3</sup>, Ming Hu<sup>1</sup>, Yuxuan Zhang<sup>1</sup>, Haochen Xue<sup>1</sup>, Zhaodong Wu<sup>2</sup>, Imran Razzak<sup>2†</sup>, Qingxia Li<sup>4†</sup>, Jionglong Su<sup>1†</sup>

<sup>1</sup> School of Artificial Intelligence and Advanced Computing, Xi'an Jiaotong-Liverpool University

<sup>2</sup> Mohamed bin Zayed University of Artificial Intelligence

<sup>3</sup> Monash University

<sup>4</sup> Fisk University

Imran.Razzak@mbzuai.ac.ae, qli@fisk.edu, Jionglong.Su@xjtlu.edu.cn

## Abstract

The rapid development of social media has significantly reshaped the dynamics of public opinion, resulting in complex interactions that traditional models fail to effectively capture. To address this challenge, we propose an innovative approach that integrates multi-dimensional Hawkes processes with Graph Neural Network, modeling opinion propagation dynamics among nodes in a social network while considering the intricate hierarchical relationships between comments. The extended multi-dimensional Hawkes process captures the hierarchical structure, multi-dimensional interactions, and mutual influences across different topics, forming a complex propagation network. Moreover, recognizing the lack of high-quality datasets capable of comprehensively capturing the evolution of public opinion dynamics, we introduce a new dataset, VISTA. It includes 159 trending topics, corresponding to 47,207 posts, 327,015 second-level comments, and 29,578 third-level comments, covering diverse domains such as politics, entertainment, sports, health, and medicine. The dataset is annotated with detailed sentiment labels across 11 categories and clearly defined hierarchical relationships. When combined with our method, it offers strong interpretability by linking sentiment propagation to the comment hierarchy and temporal evolution. Our approach provides a robust baseline for future research.

## 1 Introduction

In the era of rapidly developing social media, the transmission patterns and formation mechanisms of public opinion have undergone profound changes. Public opinion is inherently complex and multi-faceted, driven by individual behavior, social influence, and external stimuli such as news events or policy decisions. Social media platforms have transformed public discussions from unidirectional transmission via traditional media to dynamic inter-

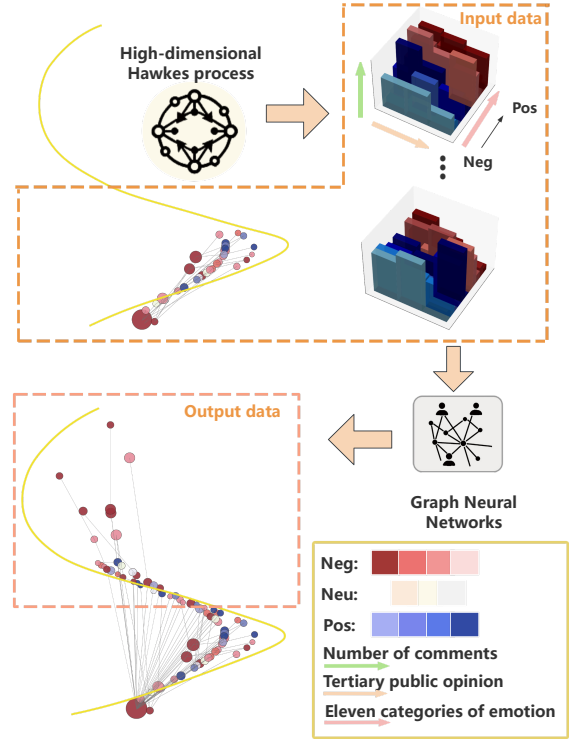


Figure 1: Opinion Dynamics Modeling illustrating two interconnected components: High-dimensional Hawkes Process (top left) and Graph Neural Network-based Sentiment Analysis (middle right).

actions among individuals, groups, and automated systems. This complexity has prompted researchers to model the dynamic process of opinion dissemination from multiple perspectives. However, existing methods still have many limitations when addressing multi-level public opinion propagation (Parsegov et al., 2016).

Opinion dynamics modeling investigates and predicts how opinions form, spread, and evolve among individuals or groups in social networks using mathematical models, computational methods, and simulation techniques. Current research faces three major challenges. First, time series-based models capture the temporal dynamics of public

opinion by forecasting changes over time. However, they overlook the hierarchical structure and complex interactions among comments. Second, network diffusion theory models the propagation paths of public opinion by representing the nodes and edges of social networks. However, most approaches assume static networks, making it difficult to capture temporal propagation dynamics. Third, although agent-based simulation models (Gürçan, 2024; Murić et al., 2022) can simulate micro-level interaction rules, their low reliance on real-world data results in limited scalability and interpretability in large-scale scenarios. To address these issues, we propose a method that integrates multidimensional Hawkes processes with Graph Neural Networks (GNNs), as illustrated in Figure 1. This approach not only accounts for the temporal dynamics of opinion propagation but also effectively simulates the interactions among nodes in social networks, particularly capturing the complex hierarchical relationships among comments.

Existing publicly available datasets on opinion propagation face significant limitations in content, structure, and temporal dimensions, restricting their application in dynamic opinion modeling. In terms of content, many datasets lack diversity and representativeness. For example, the Twitter dataset (Twitter, 2021) only includes first-level comments and retweet information, failing to reflect the complexity of multi-level opinion propagation; the Reddit dataset (Hamilton et al., 2017) provides multi-level comment information but is mainly concentrated on a few specific topics, making it difficult to cover opinion propagation patterns in different domains and scenarios. In terms of structure, many datasets do not capture the hierarchical relationships in opinion propagation. For instance, the YouTube dataset (Aliak, 2025) only records video comments and likes but lacks descriptions of tree-like hierarchical relationships between comments. Although some datasets such as FakeNewsNet (Shu et al., 2018) focus on the authenticity analysis of information dissemination, they fail to model the hierarchical structure and propagation paths of public opinion. In terms of temporal dimensions, most datasets have limited collection time spans, failing to cover the complete lifecycle of public opinion from outbreak to decline. For example, political event datasets (Conover et al., 2011) focus only on short-term political event discussions, while COVID-19 datasets (Cinelli et al., 2020) only record early pandemic opinion prop-

agation, failing to capture the long-term dynamic changes of public opinion. Additionally, on a single platform at the same time, multiple hot topics often influence each other, forming complex propagation networks. Interactions among different topics may lead to the migration of user opinions and behaviors across multiple discussions, thereby affecting the transmission patterns and evolution trajectories of public opinion. However, existing datasets generally fail to fully consider this complexity.

To solve these problems, we propose a brand new dataset that comprehensively covers multi-level comment structures and includes the mutual influence of multiple hot opinion topics. This dataset not only records the lifecycle of topics, from the outbreak to the decline of public opinion, but also considers the interactions and mutual influences among different topics, forming a complex propagation network. Additionally, the hierarchical structure of comments in the dataset adopts a tree-like relationship, which can more realistically reflect the complex interactions in opinion propagation. Based on this dataset, we propose a method combining multidimensional Hawkes processes and GNN. This method can effectively model the temporal dynamics of opinion propagation, the hierarchical relationships among comments, the complex interactions between nodes in social networks, and the interaction processes among different topics.

Our contributions are as follows:

- 1) We propose a novel approach for modeling opinion propagation by integrating multidimensional Hawkes processes with GNN. This method effectively captures temporal dynamics, hierarchical structures, and multidimensional interactions in social media discussions.
- 2) We release the VISTA dataset, a multi-scale public opinion resource that tracks the complete life cycles of 159 viral topics. The dataset includes over 500,000 hierarchically structured comments, annotated with fine-grained sentiment labels across 11 categories.
- 3) We establish a highly interpretable model that provides valuable and deep insights into the evolution of opinions in social media discussions, establishing a solid baseline for future studies using the VISTA dataset.

## 2 Related Work

Opinion propagation has evolved significantly since the mid-20th century, initially grounded in

sociological theories such as Katz and Lazarsfeld’s Two-Step Flow Theory (Katz et al., 2017), which emphasizes the role of opinion leaders in information dissemination, and Noelle-Neumann’s Spiral of Silence Theory (Noelle-Neumann, 1974), which accounts for the silence of minority opinions. With the rise of the internet, time series models such as AutoRegressive Integrated Moving Average (ARIMA) have been used to predict popularity trends in opinion events, although they struggle with nonlinear relationships (Box et al., 2015; De et al., 2016; Torres et al., 2021). The Susceptible-Infected-Recovered (SIR) model (Woo et al., 2011) is adapted for opinion propagation but assumes static networks, limiting its applicability in dynamic contexts (Anderson, 1991; Woo et al., 2011). Complex network theories, such as Barabási and Albert’s scale-free network (Barabási and Albert, 1999) as well as Watts and Strogatz’s small-world theory (Watts and Strogatz, 1998), provide further insights into network structures. However, methods such as Graph Convolutional Networks (GCNs) (Kipf and Welling, 2016) also assume static structures and cannot fully capture evolving dynamics (Kipf and Welling, 2016; Wu et al., 2020). Hierarchical models (Yang et al., 2016; Jin et al., 2014) address stepwise information spread, but lack temporal dynamics (Newman et al., 2011; Arenas et al., 2008).

From 2015 to 2020, deep learning algorithm such as LSTM and RNN models (Wu et al., 2020) achieve a breakthrough in modeling opinion propagation, capturing long-term dependencies but neglecting opinion structure. GNNs (Longa et al., 2023) aim to model both temporal and structural evolution, but challenges still remain in multi-level propagation (Longa et al., 2023; Kazemi et al., 2020). Graph Attention Networks (GATs) and other models (Rath et al., 2021) have improved predictive performance, with recent research increasingly focused on multi-dimensional aspects, including temporal dynamics, hierarchical structures, and emotional diffusion (Chen et al., 2023). Cross-topic propagation models gain attention during the COVID-19 pandemic, examining the timing and sequencing of social media posts (Yin et al., 2020), but unified frameworks integrating these multi-dimensional features are still lacking (Parsegov et al., 2016; Cao et al., 2019). Agent-based simulations, while useful for modeling complex behaviors, face scalability and validation challenges (Gürçan, 2024; Murić et al., 2022; Epstein, 2012).

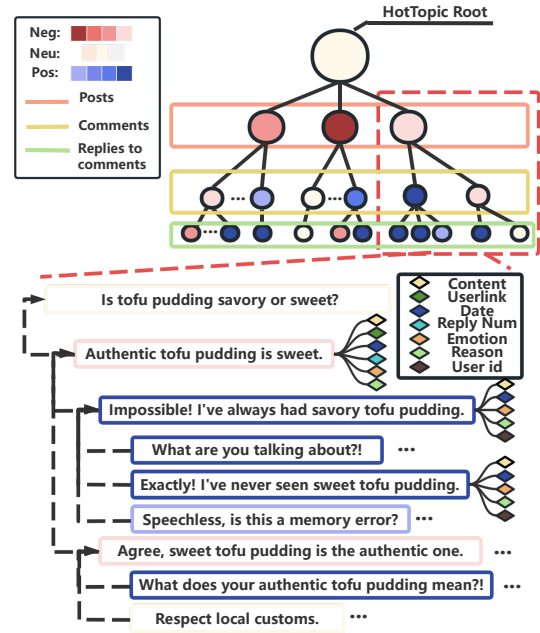


Figure 2: Illustrative Diagram of VISTA Datasets. The replies to comments, comments, and posts together form a complete opinion event in our dataset.

Despite significant progress, a unified method to simultaneously capture temporal, structural, and multi-dimensional features in opinion propagation remains an open challenge.

### 3 Dataset Construction

To support research on opinion propagation, we collect real-time comments and interaction records from Weibo (Weibo, n.d.) related to trending events, spanning from 2024 to early 2025. Using specified keywords and event lists, we capture the full opinion cycle, from event inception to attention decline. After data merging, we perform deduplication, standardize formats, and apply a custom dictionary and multilingual detection to remove irrelevant or anomalous comments. We also filter out sensitive personal information. Finally, timestamps are standardized for temporal analysis and hierarchical structure construction.

To retain the content of comments, we reconstruct the tree-like structure of comments and replies by recording and correcting the parent comment IDs. Using hash mapping and indexing, we match each comment with its parent, tracing back layer by layer to the deepest child comment while limiting the depth to a maximum of three levels. This three-level structure captures opinions on posts, comments, and supporting or opposing voices, providing an efficient and comprehensive

Category	Type	Emotion classification											Total	
		A	An	S	F	C	N	Ca	O	H	Ex	El		
Basic	P	Normal	2529	4479	3362	1866	1552	3773	429	11469	9784	7343	621	47207
		Abnormal	0	0	0	0	0	0	0	0	0	0	0	0
	C	Normal	11738	10477	8398	9354	5409	34412	4447	74039	57331	37178	12587	265370
		Abnormal	1911	1829	1006	1549	1056	10873	647	17443	13484	9574	2273	61645
	R	Normal	2670	2145	619	1044	695	10318	188	2616	3341	1276	45	24957
		Abnormal	343	256	49	150	162	2024	10	564	721	305	37	4621
Social	CL	Normal	407	468	311	533	115	1038	96	2856	1265	1227	161	8477
		Abnormal	50	121	60	64	44	236	17	856	495	365	74	2382
	RL	Normal	1680	1095	287	641	357	3730	70	964	1171	402	16	10413
		Abnormal	231	111	25	94	38	710	2	160	241	84	12	1708

\*The dataset used in this study does not contain any fake accounts (or astroturfing)

\*P:posts. C:comments. R:replies. CL:comments with likes. RL:replies with likes.

\*A:Angry, An:Anxious, S:Sad, F:Frustrated, C:Consoling, N:Neutral, Ca:Calm, O:Optimistic, H:Happy, Ex:Excited, El:Elated

Table 1: Statistics of VISTA Dataset

Dataset	Md	Cd	Lt	Cpoe	El
Twitter Dataset	✓	✓	✗	✗	✓*
Reddit Dataset	✓	✓	✗	✗	✗
YouTube Dataset	✓	✓	✗	✗	✗
FakeNewsNet Dataset	✗	✗	✓	✗	✓
Political Event Dataset	✗	✗	✗	✗	✗
COVID-19 Dataset	✗	✗	✓	✗	✗
<b>Ours</b>	✓	✓	✓	✓	✓

Md: Multilevel data. Cd: Content diversity. Lt: Length of time. Cpoe: Complete public opinion event. El: Emotional label. \*:Partial annotation

Table 2: Multidimensional comparison of datasets

representation of opinion propagation. In cases where parent IDs are missing or refer to deleted comments, we treat them as top-level comments and mark them separately. After this process, the comment data forms directed trees, with each comment assigned an accurate hierarchical label. As illustrated in Figure 2, the VISTA dataset captures the full structure of opinion events, including replies, comments, and posts. The dataset’s statistical breakdown, categorized by comment levels and emotional annotations, is provided in Table 1.

For sentiment and event label generation, we use the GLM-4-plus model for automated comment annotation, yielding 11 sentiment levels categorized into negative, neutral, and positive, along with the model’s rationale. To ensure annotation reliability, we first manually label a subset of high-quality comments, using them for prompt engineering and fine-tuning before applying batch inference to the remaining comments. During a secondary review, significant discrepancies with manual annotations are corrected. Finally, spot checks are performed to verify dataset quality, achieving a mean Cohen’s Kappa of 0.85 for sentiment annotation across ten final checks. We compare the multidimensional aspects of various opinion propagation datasets

in Table 2, highlighting their strengths and limitations. Event labels are also assigned to each comment, along with user attributes, ensuring traceability within the social network and public opinion context.

## 4 Task Definition

Suppose there are  $M$  parallel “hot topics” in a given time period, each represented by a root post  $H_m$  for  $m \in \{1, \dots, M\}$ . Under these root posts, users continuously produce hierarchical comments: if a comment replies directly to a hot topic, it is considered level 1; if it replies to a comment at the previous level, it spawns a new node in that thread, increasing the level by 1. Formally, we denote each observed comment event as

$$\mathcal{E} = \{e_i \mid e_i = (h_i, l_i, p_i, t_i)\},$$

where  $h_i \in \{1, \dots, M\}$  indicates the hot topic to which the comment belongs ( $i$  represents an individual comment event, which includes its topic, level, parent comment, and timestamp),  $l_i \geq 1$  is the comment’s level within that topic,  $p_i$  is the parent comment or root post, and  $t_i$  is the posting timestamp.

Because multiple hot topics may exhibit mutual influence (for example, content overlap or shared user bases across different topics), comment evolution can manifest both *cross-topic* mutual excitation and *hierarchical expansion* within each individual chain. Therefore, given a historical comment event set  $\mathcal{E}_{\leq T}$  (i.e., all comments observed up to some time  $T$ ), our goal is to learn a predictive function

$$F(\mathcal{E}_{\leq T}) \mapsto \hat{\mathcal{E}}_{>T},$$

where  $\mathcal{E}_{\leq T}$  denotes all observed comments at or before  $T$ , and  $\hat{\mathcal{E}}_{>T}$  denotes the predicted comments

that may appear during the future time interval  $(T, T + \Delta]$ .

Concretely, the prediction covers two complementary dimensions:

- **Temporal dimension**, it focuses on predicting when new comments will emerge and how the volume of comments will change over time across various topics and hierarchical levels.
- **Structural dimension**, it focuses on how newly added comments connect to parent nodes, potentially spanning diverse topics or levels, thus driving the dynamic evolution of the hierarchical structure.

The core of the task lies in simultaneously accounting for cascading responses within the hierarchical structure (where higher-level comments trigger replies at subsequent levels) and sentiment propagation patterns to provide a comprehensive prediction of future comment behavior. This requires not only modeling the dynamic temporal and structural evolution of the discussion network but also effectively capturing how sentiment propagates through comments, enabling more accurate forecasting of the evolution of public opinion on social media platforms.

## 5 Methodology

As illustrated in Figure 3, the architecture of our Social Network Sentiment Analysis model combines a high-dimensional Hawkes process with a graph neural network to model sentiment dynamics.

Our method integrates multi-level comments with fine-grained sentiment levels. When incorporating the Hawkes process into sentiment modeling, the main challenge lies in obtaining direct predictions for the number of comments associated with different sentiment opinions. To address this, we model the Hawkes process in higher dimensions by combining hierarchy and sentiment levels as two discrete attributes. Each dimension corresponds to a specific “(hierarchy, sentiment level)” pair, enabling the intensity function to estimate the number of comments associated with various sentiment opinions. The high-dimensional Hawkes process captures the temporal evolution of comments under different sentiment labels and hierarchy levels. The output is then used to construct a GNN, further capturing the dynamic propagation structure and sentiment diffusion patterns among comments.

Let  $l$  denote the hierarchy level and  $c$  denote the sentiment level, where there are  $L$  hierarchy levels

and  $C$  sentiment levels. In this paper,  $L = 3$  and  $C = 11$ . Each comment is mapped to a dimension  $\omega = (l, c)$ , where  $1 \leq l \leq L$  and  $1 \leq c \leq C$ . The Cartesian product of hierarchy levels and sentiment levels forms a new set of dimensions:

$$\Omega = \{(l, c) \mid l \in \{1, \dots, L\}, c \in \{1, \dots, C\}\},$$

where  $\Omega$  represents all possible combinations of hierarchy levels and sentiment levels, and  $\omega \in \Omega$  corresponds to a specific type of event. If a comment occurs at time  $t_i^\omega$ , then it is assigned to dimension  $\omega$ . Based on this, the intensity function of the high-dimensional Hawkes process is defined as:

$$\lambda_\omega(t) = \mu_\omega + \sum_{\omega' \in \Omega} \sum_{t_j^{\omega'} \leq t} \alpha_{\omega, \omega'} \phi_{\omega, \omega'}(t - t_j^{\omega'}), \quad (1)$$

where  $\mu_\omega$  denotes the baseline arrival rate for dimension  $\omega$ ,  $\alpha_{\omega, \omega'}$  measures the excitation strength from dimension  $\omega'$  to dimension  $\omega$ , and  $\phi_{\omega, \omega'}(\tau)$  is the decay kernel function. In this case, the decay kernel function is defined as an exponential kernel,  $\phi_{\omega, \omega'}(\tau) = e^{-\beta_{\omega, \omega'} \tau} \mathbf{1}_{\{\tau \geq 0\}}$ , where  $\beta_{\omega, \omega'}$  is the decay coefficient and  $\mathbf{1}_{\{\tau \geq 0\}}$  is indicator function.

To estimate  $\mu_\omega$ ,  $\alpha_{\omega, \omega'}$ , and  $\beta_{\omega, \omega'}$ , we employ the maximum likelihood method. Given an observation window  $[0, T]$ , let  $\{t_1^\omega, t_2^\omega, \dots, t_{N_\omega}^\omega\}$  denote the occurrence times of all events (comments) in dimension  $\omega$ , with  $N_\omega$  being the total number of events. The log-likelihood function of the high-dimensional Hawkes process is expressed as:

$$\mathcal{L} = \sum_{\omega \in \Omega} \left[ \sum_{i=1}^{N_\omega} \ln(\lambda_\omega(t_i^\omega)) - \int_0^T \lambda_\omega(t) dt \right], \quad (2)$$

where  $T$  is the end of the observation window.

### Log-likelihood and Gradient Derivations

The parameters to be learned are:

$$\theta = \{ \{\mu_\omega\}_{\omega \in \Omega}, \{\alpha_{\omega, \omega'}\}_{\omega, \omega' \in \Omega}, \{\beta_{\omega, \omega'}\}_{\omega, \omega' \in \Omega} \}. \quad (3)$$

The gradient of  $\mathcal{L}$  taken with respect to  $\mu_\omega$  is:

$$\frac{\partial \mathcal{L}}{\partial \mu_\omega} = \sum_{i=1}^{N_\omega} \frac{1}{\lambda_\omega(t_i^\omega)} - \int_0^T 1 dt = \sum_{i=1}^{N_\omega} \frac{1}{\lambda_\omega(t_i^\omega)} - T. \quad (4)$$

For the gradient with respect to  $\alpha_{\omega, \omega'}$ , it includes the log term and the integral term. The gradient of the log term can be calculated as:

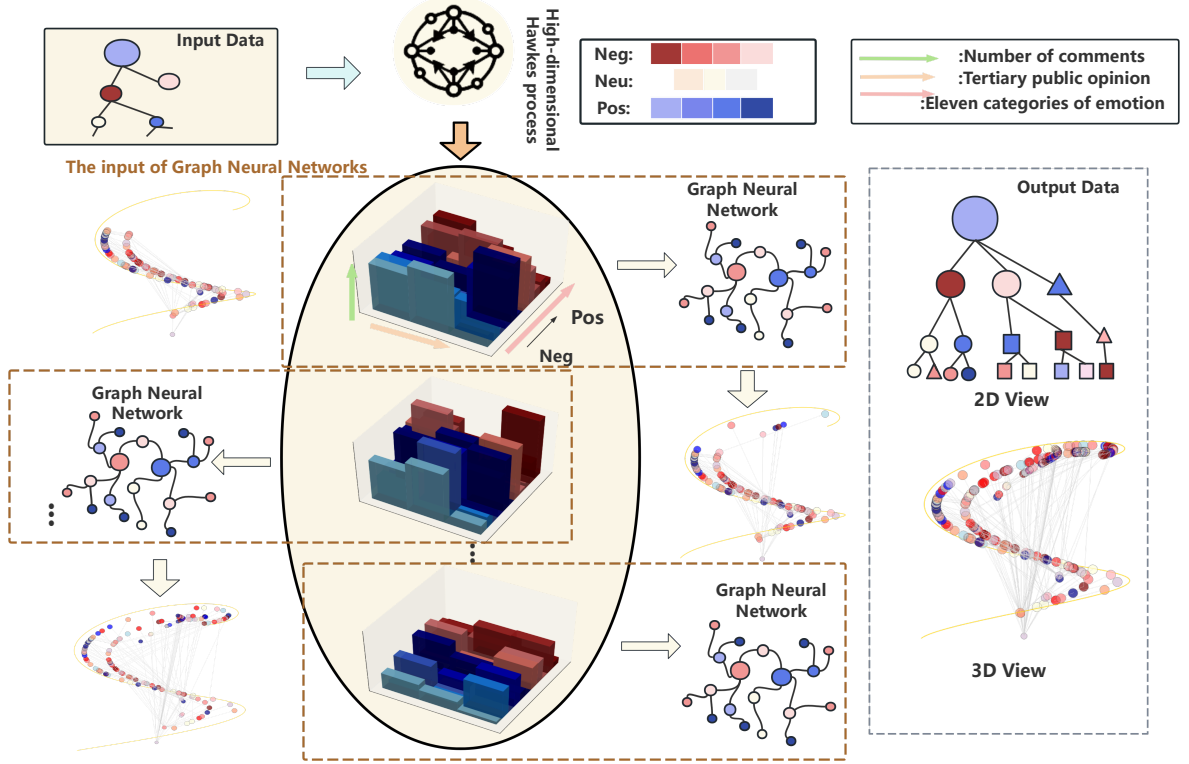


Figure 3: Architecture of the Social Network Sentiment Analysis Model. Our framework analyzes sentiment in social networks using a high-dimensional Hawkes process and graph neural networks. The Hawkes process predicts comment volume and sentiment, while GNN learns the social structure, classifies nodes, and constructs a predicted network. Through iterations, the framework achieves sentiment analysis.

$$\sum_{i=1}^{N_{\omega}} \ln(\lambda_{\omega}(t_i^{\omega})) \rightarrow \sum_{i=1}^{N_{\omega}} \frac{1}{\lambda_{\omega}(t_i^{\omega})} \cdot \frac{\partial}{\partial \alpha_{\omega, \omega'}} \lambda_{\omega}(t_i^{\omega}). \quad (5)$$

For a detailed mathematical proof, refer to Appendix Section 9.2.

Using Equation (1), we derive:

$$\frac{\partial}{\partial \alpha_{\omega, \omega'}} \lambda_{\omega}(t_i^{\omega}) = \sum_{j=1}^{N_{\omega'}} e^{-\beta_{\omega, \omega'}(t_i^{\omega} - t_j^{\omega'})} \mathbf{1}_{\{t_j^{\omega'} < t_i^{\omega}\}}. \quad (6)$$

where  $N_{\omega'}$  is the total number of events of type  $\omega'$  in the observed time window  $[0, T]$ .

The integral term can be rewritten as:

$$\begin{aligned} \int_0^T \partial_{\alpha} \lambda_{\omega}(t) dt &= \sum_{j=1}^{N_{\omega'}} \int_{t_j^{\omega'}}^T \partial_{\alpha} \left( \alpha_{\omega, \omega'} e^{-\beta_{\omega, \omega'}(t - t_j^{\omega'})} \right) dt \\ &= \sum_{j=1}^{N_{\omega'}} \int_{t_j^{\omega'}}^T e^{-\beta_{\omega, \omega'}(t - t_j^{\omega'})} dt \\ &= \sum_{j=1}^{N_{\omega'}} \frac{1}{\beta_{\omega, \omega'}} \left[ 1 - e^{-\beta_{\omega, \omega'}(T - t_j^{\omega'})} \right]. \quad (7) \end{aligned}$$

where  $\partial_{\alpha} \equiv \frac{\partial}{\partial \alpha_{\omega, \omega'}}$ .

Combining the terms, we can arrive at the gradient with respect to  $\alpha_{\omega, \omega'}$  as:

$$\begin{aligned} \frac{\partial \mathcal{L}}{\partial \alpha_{\omega, \omega'}} &= \sum_{i=1}^{N_{\omega}} \frac{1}{\lambda_{\omega}(t_i^{\omega})} \sum_{j=1}^{N_{\omega'}} e^{-\beta_{\omega, \omega'}(t_i^{\omega} - t_j^{\omega'})} \mathbf{1}_{\{t_j^{\omega'} < t_i^{\omega}\}} \\ &\quad - \sum_{j=1}^{N_{\omega'}} \frac{1}{\beta_{\omega, \omega'}} \left[ 1 - e^{-\beta_{\omega, \omega'}(T - t_j^{\omega'})} \right]. \quad (8) \end{aligned}$$

For a detailed mathematical proof, refer to Appendix Section 9.3. The gradient with respect to  $\beta_{\omega, \omega'}$  follows a similar derivation. For a detailed mathematical proof, refer to Appendix Section 9.4.

For the Hawkes process to remain stable and avoid exponential growth, the following stability condition is required for each dimension  $\omega$ :

$$\sum_{\omega' \in \Omega} \frac{\alpha_{\omega, \omega'}}{\beta_{\omega, \omega'}} < 1. \quad (9)$$

Otherwise, it leads to a critical or supercritical state, resulting in exponential comment growth and loss of stationarity.

### Prediction of Comment Counts

To predict the number of comments for a specific hierarchy-sentiment pair within the interval  $[T, T + \Delta]$ , we integrate the intensity function over the interval. For any  $\omega = (l, c)$ , the expected number of events occurring within  $[T, T + \Delta]$  is given by:

$$\hat{N}_\omega(T, T + \Delta) = \int_T^{T+\Delta} \lambda_\omega(t) dt. \quad (10)$$

For scenarios focusing on all sentiment levels within a specific hierarchy level or all hierarchy levels within a specific sentiment level, the predictions for the corresponding dimensions  $\omega$  are aggregated accordingly. The high-dimensional Hawkes model is trained using stochastic gradient methods, enabling the simultaneous estimation of all parameters  $\mu_\omega$ ,  $\alpha_{\omega, \omega'}$ , and  $\beta_{\omega, \omega'}$ . This framework facilitates both independent and combined calculations of intensities across dimensions during inference or prediction.

### Graph Neural Network Modeling

The GNN models the evolution of opinion propagation. Its primary tasks are node classification and edge prediction. Node classification aims to predict the sentiment level of each comment node, while edge prediction seeks to infer the propagation paths and their strengths between comments. Based on the predicted comments and their sentiment distributions generated by the high-dimensional Hawkes process, we construct an opinion propagation graph, denoted as  $\mathcal{G} = (\mathcal{V}, \mathcal{E})$ , where  $\mathcal{V}$  represents the set of comment nodes, and  $\mathcal{E}$  represents the parent-child relationships between comments.

Each node's features are composed of the intensity function values  $\lambda_\omega(t)$  generated by the Hawkes process and the sentiment distribution  $q_c(v)$ . Here,  $\lambda_\omega(t)$  represents the arrival intensity of the comment, and  $q_c(v)$  denotes the probability that node  $v$  belongs to sentiment level  $c \in \{1, 2, \dots, C\}$ . Specifically, the sentiment distribution is defined as:

$$q_c(v) = \frac{\lambda_{(l,c)}(t)}{\sum_{c'=1}^C \lambda_{(l,c')}(t)}, \quad (11)$$

where  $\lambda_{(l,c)}(t)$  is the intensity function value at time  $t$  for hierarchy level  $l$  and sentiment level  $c$ , and  $C$  is the total number of sentiment categories. This distribution captures the sentiment inclination of the node. The edge features  $\mathbf{e}_{uv}$  include the time difference between nodes,  $\Delta t = t_v - t_u$ ,  $\Delta t > 0$ , and the excitation strength  $\alpha_{\omega, \omega'}$ . The former measures

the time interval between comments, while the latter reflects the propagation relationships between different sentiments and hierarchy levels.

In the graph, node embeddings are updated using a message-passing mechanism. Let  $t$  denote the current time slice and the embedding of node  $v$  be defined as  $\mathbf{h}_v^{(t)}$ . The updated rule for node embeddings is:

$$\mathbf{h}_v^{(t+1)} = \sigma \left( \mathbf{W}_1 \mathbf{h}_v^{(t)} + \sum_{u \in \mathcal{N}(v)} \mathbf{W}_2 \mathbf{e}_{uv} \mathbf{h}_u^{(t)} \right), \quad (12)$$

where  $\mathbf{h}_v^{(t+1)}$  is the embedding of node  $v$  at time  $t + 1$ ,  $\mathcal{N}(v)$  is the set of neighbors of node  $v$ ,  $\mathbf{e}_{uv}$  is the feature vector of edge  $(u, v)$ ,  $\mathbf{W}_1, \mathbf{W}_2$  are learnable linear transformation matrices, and  $\sigma(\cdot)$  is a non-linear activation function. This update formula aggregates features dynamically by combining historical embeddings of the node itself with embeddings of its neighbors, weighted by the edge features.

Based on the updated node embeddings, we classify the sentiment level of each node using the following formula:

$$P(c | v) = \text{softmax}(\mathbf{W}_c \mathbf{h}_v^{(t+1)}), \quad (13)$$

where  $\mathbf{W}_c$  is the linear transformation matrix for sentiment classification, and  $P(c | v)$  represents the predicted probability that node  $v$  belongs to sentiment level  $c$ .

To optimize the accuracy of node classification and edge prediction, we introduce two loss functions: the sentiment prediction loss  $\mathcal{L}_{\text{sentiment}}$  and the graph structure loss  $\mathcal{L}_{\text{struct}}$ . The sentiment prediction loss measures the accuracy of the predicted sentiment distribution for nodes and is defined as:

$$\mathcal{L}_{\text{sentiment}} = - \sum_{v \in \mathcal{V}_{\text{pred}}} \sum_{c=1}^C q_c(v) \cdot \ln P(c | v), \quad (14)$$

where  $\mathcal{V}_{\text{pred}}$  denotes the set of nodes predicted by the Hawkes process, and  $q_c(v)$  is the normalized sentiment distribution output from the Hawkes process, representing the true sentiment label of node  $v$ .

The graph structure loss measures the structural differences between the predicted graph  $\mathcal{G}_{\text{pred}}$  and the true graph  $\mathcal{G}_{\text{true}}$ . It is defined as:

$$\mathcal{L}_{\text{struct}} = \sum_{(u,v) \in \mathcal{E}} |e_{uv}^{\text{pred}} - e_{uv}^{\text{true}}|, \quad (15)$$

where  $\mathcal{E}$  is the set of edges in the graph, and  $e_{uv}^{\text{pred}}$  and  $e_{uv}^{\text{true}}$  represent the feature values of edge  $(u, v)$  in the predicted graph and the true graph, respectively, reflecting the differences in propagation paths.

The final optimization objective combines the two losses, and the composite loss function is defined as:

$$\mathcal{L}_{\text{total}} = \lambda_1 \mathcal{L}_{\text{sentiment}} + \lambda_2 \mathcal{L}_{\text{struct}}, \quad (16)$$

where  $\lambda_1$  and  $\lambda_2$  are hyperparameters that control the weights of the sentiment loss and the structure loss, respectively. By minimizing  $\mathcal{L}_{\text{total}}$ , the graph neural network optimizes the performance of both node classification and edge prediction, thereby capturing the dynamic evolution of opinion propagation in terms of both temporal and structural dimensions.

## 6 Evaluation Metrics

**Sentiment Prediction Accuracy (SA):** The sentiment prediction accuracy measures how well the model predicts the sentiment label for each comment. Given the true sentiment label  $c(v)$  and the predicted sentiment label  $\hat{c}(v)$  for each comment node  $v$ , the sentiment prediction accuracy  $\text{Acc}_{\text{sentiment}}$  is defined as:

$$\text{Acc}_{\text{sentiment}} = \frac{1}{N} \sum_{v \in \mathcal{V}} \mathbf{1}(\hat{c}(v) = c(v))$$

where  $\mathbf{1}(\cdot)$  is an indicator function that equals 1 when the predicted sentiment matches the true sentiment, and 0 otherwise.

**Structural Consistency Prediction Accuracy (SCA):** The structural consistency prediction accuracy measures how well the model predicts the hierarchical structure of comments. Specifically, it checks whether the set of child nodes for each parent node is correctly predicted. The structural consistency prediction accuracy  $\text{Acc}_{\text{structure}}$  is defined as:

$$\text{Acc}_{\text{structure}} = \frac{1}{|\mathcal{V}_{\text{true}}|} \sum_{v \in \mathcal{V}_{\text{true}}} \mathbf{1}(\mathcal{C}_v^{\text{pred}} = \mathcal{C}_v^{\text{true}})$$

where  $\mathcal{C}_v^{\text{true}}$  and  $\mathcal{C}_v^{\text{pred}}$  are the sets of child nodes of the parent node  $v$  in the true and predicted graphs, respectively.

## 7 Experiments

### 7.1 Dataset

To ensure the reliability and fairness of the experimental results, we divide the VISTA dataset into training, validation, and test sets. Specifically, 127 trending topics are used for training the model, covering all topics and levels of comments to ensure the model can learn diverse opinion chain features. Both the validation and test sets consist of 16 trending topics each.

### 7.2 Baseline for Dynamic Propagation

Table 3 gives the performance evaluation of the model on the future opinion chain prediction task at three data proportions (15%, 20%, and 25%). As the data proportion increases, both Sentiment Prediction Accuracy and Structural Consistency Prediction Accuracy performance consistently improve, indicating that a larger dataset effectively enhances the model’s predictive capabilities. This table provides the baseline performance of our model on the VISTA dataset, confirming the significant impact of data volume on prediction accuracy.

Data Proportion	SA (Val/Test %)	SCA (Val/Test %)
15%	19.75/18.31	23.41/21.22
20%	24.12/22.19	29.34/26.98
25%	29.31/26.99	37.29/35.76

Table 3: Performance of Future Opinion Chain Prediction with Different Data Proportions. This table presents the evaluation of the model’s performance on future opinion chain prediction tasks, based on three different data proportions: 15%, 20%, and 25%.

## 8 Conclusion

In conclusion, we propose a novel and highly interpretable method that combines high-dimensional Hawkes processes with Graph Neural Networks for modeling opinion propagation on social media. By introducing the VISTA dataset, which includes multi-level comment structures, sentiment annotations, and interactions between trending topics, we provide valuable research data for future studies on opinion dynamics. Our method effectively captures the temporal evolution, structural changes, and sentiment diffusion patterns in discussions. In the future, we plan to apply more advanced methods on this dataset to further explore the underlying mechanisms of opinion dynamics.



## Limitations

Although this study provides valuable insights, there are still some limitations. Our data is limited to Weibo, which may restrict the generalizability of the conclusions, as user behavior may differ across various social platforms and cultural contexts. Additionally, we assume that the data points are independent; however, in practice, interactions within Weibo’s fan communities and the self-organized moderation of comments may lead to data correlations, impacting the accuracy of the model. We also assume that the data collection process is noise-free, but in reality, noise and manipulation could affect the reliability of the results. While we have adopted an interpretable model to ensure transparency, this may limit the model’s predictive performance, especially when dealing with more complex data. The model may be overly sensitive to Weibo-specific data characteristics, resulting in limited generalizability. We have decided to make all our code publicly available for other researchers to validate and reproduce our experimental results. Future research will consider validating our model on more platforms and datasets to further improve its robustness and generalizability.

## References

- Atif Aliak. 2025. [Youtube comments dataset](https://www.kaggle.com/datasets/atifaliak/youtube-comments-dataset). <https://www.kaggle.com/datasets/atifaliak/youtube-comments-dataset>. Accessed: 2025-02-12.
- RM Anderson. 1991. *Infectious diseases of humans: dynamics and control*. Oxford University Press.
- Alex Arenas, Albert Díaz-Guilera, Jurgen Kurths, Yamir Moreno, and Changsong Zhou. 2008. Synchronization in complex networks. *Physics reports*, 469(3):93–153.
- Albert-László Barabási and Réka Albert. 1999. Emergence of scaling in random networks. *science*, 286(5439):509–512.
- George EP Box, Gwilym M Jenkins, Gregory C Reinsel, and Greta M Ljung. 2015. *Time series analysis: forecasting and control*. John Wiley & Sons.
- Yan Cao, Yihong Dong, Shaoqing Wu, Yu Xin, and Jiangbo Qian. 2019. Dynamic network embedding for link prediction. In *2019 IEEE Intl Conf on Parallel & Distributed Processing with Applications, Big Data & Cloud Computing, Sustainable Computing & Communications, Social Computing & Networking (ISPA/BDCloud/SocialCom/SustainCom)*, pages 920–927. IEEE.
- Zhihao Chen, Bingbing Xu, Tiecheng Cai, Zhou Yang, and Xiangwen Liao. 2023. A dynamic emotional propagation model over time for competitive environments. *Electronics*, 12(24):4937.
- Matteo Cinelli, Walter Quattrociocchi, Alessandro Galeazzi, Carlo Michele Valensise, Emanuele Brugnoli, Ana Lucia Schmidt, Paola Zola, Fabiana Zollo, and Antonio Scala. 2020. The covid-19 social media infodemic. *Scientific reports*, 10(1):1–10.
- Michael Conover, Jacob Ratkiewicz, Matthew Francisco, Bruno Gonçalves, Filippo Menczer, and Alessandro Flammini. 2011. Political polarization on twitter. In *Proceedings of the international aaai conference on web and social media*, volume 5, pages 89–96.
- Abir De, Isabel Valera, Niloy Ganguly, Sourangshu Bhattacharya, and Manuel Gomez Rodriguez. 2016. *c. Advances in neural information processing systems*, 29.
- Joshua M Epstein. 2012. *Generative social science: Studies in agent-based computational modeling*. Princeton University Press.
- Önder Gürcan. 2024. Llm-augmented agent-based modelling for social simulations: Challenges and opportunities. *HHAI 2024: Hybrid Human AI Systems for the Social Good*, pages 134–144.
- Will Hamilton, Zhitao Ying, and Jure Leskovec. 2017. Inductive representation learning on large graphs. *Advances in neural information processing systems*, 30.
- Zhiwei Jin, Juan Cao, Yu-Gang Jiang, and Yongdong Zhang. 2014. News credibility evaluation on microblog with a hierarchical propagation model. In *2014 IEEE international conference on data mining*, pages 230–239. IEEE.
- Elihu Katz, Paul F Lazarsfeld, and Elmo Roper. 2017. *Personal influence: The part played by people in the flow of mass communications*. Routledge.
- Seyed Mehran Kazemi, Rishab Goel, Kshitij Jain, Ivan Kobyzev, Akshay Sethi, Peter Forsyth, and Pascal Poupart. 2020. Representation learning for dynamic graphs: A survey. *Journal of Machine Learning Research*, 21(70):1–73.
- Thomas N Kipf and Max Welling. 2016. Semi-supervised classification with graph convolutional networks. *arXiv preprint arXiv:1609.02907*.
- Antonio Longa, Veronica Lachi, Gabriele Santin, Monica Bianchini, Bruno Lepri, Pietro Lio, Franco Scarselli, and Andrea Passerini. 2023. Graph neural networks for temporal graphs: State of the art, open challenges, and opportunities. *arXiv preprint arXiv:2302.01018*.
- Goran Murić, Alexey Tregubov, Jim Blythe, Andrés Abeliuk, Divya Choudhary, Kristina Lerman, and Emilio Ferrara. 2022. Large-scale agent-based simulations of online social networks. *Autonomous Agents and Multi-Agent Systems*, 36(2):38.

- Mark Newman, Albert-László Barabási, and Duncan J Watts. 2011. *The structure and dynamics of networks*. Princeton university press.
- Elisabeth Noelle-Neumann. 1974. The spiral of silence a theory of public opinion. *Journal of communication*, 24(2):43–51.
- Sergey E Parsegov, Anton V Proskurnikov, Roberto Tempo, and Noah E Friedkin. 2016. Novel multi-dimensional models of opinion dynamics in social networks. *IEEE Transactions on Automatic Control*, 62(5):2270–2285.
- Bhavtosh Rath, Xavier Morales, and Jaideep Srivastava. 2021. Scarlet: explainable attention based graph neural network for fake news spreader prediction. In *Pacific-Asia conference on knowledge discovery and data mining*, pages 714–727. Springer.
- Kai Shu, Deepak Mahudeswaran, Suhang Wang, Dongwon Lee, and Huan Liu. 2018. Fakenewsnet: A data repository with news content, social context and dynamic information for studying fake news on social media. *arXiv preprint arXiv:1809.01286*.
- José F Torres, Dalil Hadjout, Abderrazak Sebaa, Francisco Martínez-Álvarez, and Alicia Troncoso. 2021. Deep learning for time series forecasting: a survey. *Big Data*, 9(1):3–21.
- Twitter. 2021. [Twitter dataset for sentiment analysis. https://www.kaggle.com/datasets/jp797498e/twitter-entity-sentiment-analysis.](https://www.kaggle.com/datasets/jp797498e/twitter-entity-sentiment-analysis) Accessed: 2025-02-12.
- Duncan J Watts and Steven H Strogatz. 1998. Collective dynamics of ‘small-world’ networks. *nature*, 393(6684):440–442.
- Weibo. n.d. [Weibo](#). Accessed: 2024-12-30.
- Jiyoung Woo, Jaebong Son, and Hsinchun Chen. 2011. An sir model for violent topic diffusion in social media. In *Proceedings of 2011 IEEE International Conference on Intelligence and Security Informatics*, pages 15–19. IEEE.
- Zonghan Wu, Shirui Pan, Fengwen Chen, Guodong Long, Chengqi Zhang, and S Yu Philip. 2020. A comprehensive survey on graph neural networks. *IEEE transactions on neural networks and learning systems*, 32(1):4–24.
- Zichao Yang, Diyi Yang, Chris Dyer, Xiaodong He, Alex Smola, and Eduard Hovy. 2016. Hierarchical attention networks for document classification. In *Proceedings of the 2016 conference of the North American chapter of the association for computational linguistics: human language technologies*, pages 1480–1489.
- Fulian Yin, Xueying Shao, Meiqi Ji, and Jianhong Wu. 2020. Quantify influence of delay in opinion transmission of opinion leaders on covid-19 information propagation in the chinese sina-microblog. *arXiv preprint arXiv:2011.06797*.

## 9 Appendix

### 9.1 Ethics Statements

The dataset used in our study is collected in compliance with ethical research guidelines, ensuring that user privacy and data security are adequately protected. The data primarily consists of social media discussions, including posts, comments, and replies, annotated with multiple emotional categories. To minimize risks associated with sensitive content, we implement a multi-stage filtering process to remove personally identifiable information, explicit material, and offensive language. However, due to the inherent limitations of automated and manual inspection, some residual content may persist, making complete elimination a challenging task.

Since the dataset originates from real-world social interactions, it may include a small amount of misinformation or subjective opinions, which could influence analytical outcomes and model performance. We release this dataset exclusively for research purposes, aiming to support studies in opinion dynamics, sentiment analysis, and social network modeling. Researchers using this dataset should exercise caution and adhere to ethical guidelines when interpreting the results.

Our goal is to contribute to the advancement of computational social science and machine learning while ensuring responsible data usage. In future updates, we will continue to expand and refine the dataset, improving both its coverage and filtering mechanisms to enhance its reliability and applicability in diverse research scenarios.

### 9.2 A

Given the high-dimensional Hawkes process intensity function  $\lambda_\omega(t)$ , the log-likelihood function is defined as:

$$\mathcal{L} = \sum_{\omega \in \Omega} \left[ \sum_{i=1}^{N_\omega} \ln(\lambda_\omega(t_i^\omega)) - \int_0^T \lambda_\omega(t) dt \right], \quad (17)$$

where  $t_i^\omega$  is the  $i$ -th event time in the  $\omega$ -th dimension.

The intensity function  $\lambda_\omega(t)$  is composed of two terms: the first term  $\sum_{i=1}^{N_\omega} \ln(\lambda_\omega(t_i^\omega))$  is the log-likelihood of the observed event times  $t_i^\omega$ , and the second term  $\int_0^T \lambda_\omega(t) dt$  is the integral of the intensity function  $\lambda_\omega(t)$  over the time interval  $[0, T]$ , representing the expected number of events.

The intensity function for the high-dimensional Hawkes process is defined as:

$$\lambda_\omega(t) = \mu_\omega + \sum_{\omega' \in \Omega} \sum_{t_j^{\omega'} \leq t} \alpha_{\omega, \omega'} \phi_{\omega, \omega'}(t - t_j^{\omega'}), \quad (18)$$

where  $\mu_\omega$  is the baseline intensity, representing the event rate in the absence of any historical events,  $\alpha_{\omega, \omega'}$  is the excitation strength from event type  $\omega'$  to  $\omega$ , and  $\phi_{\omega, \omega'}(t - t_j^{\omega'})$  is the decay kernel, typically in the form of an exponential decay.

We need to compute the gradient of the log-likelihood function with respect to  $\mu_\omega$ :

$$\frac{\partial \mathcal{L}}{\partial \mu_\omega}. \quad (19)$$

The gradient with respect to  $\mu_\omega$  is derived in two parts. First, we consider the left part:

$$\sum_{i=1}^{N_\omega} \ln(\lambda_\omega(t_i^\omega)). \quad (20)$$

By taking the partial derivative with respect to  $\mu_\omega$  using the chain rule, we obtain that:

$$\frac{\partial}{\partial \mu_\omega} \ln(\lambda_\omega(t_i^\omega)) = \frac{1}{\lambda_\omega(t_i^\omega)} \cdot \frac{\partial \lambda_\omega(t_i^\omega)}{\partial \mu_\omega}. \quad (21)$$

Since  $\lambda_\omega(t)$  only involves  $\mu_\omega$  in the first term (i.e.,  $\mu_\omega$  only affects the baseline part of the intensity function), it yields that

$$\frac{\partial \lambda_\omega(t)}{\partial \mu_\omega} = 1. \quad (22)$$

Therefore, for each event  $t_i^\omega$ , we conclude:

$$\frac{\partial}{\partial \mu_\omega} \ln(\lambda_\omega(t_i^\omega)) = \frac{1}{\lambda_\omega(t_i^\omega)}. \quad (23)$$

Summing over all  $i$ , we get:

$$\sum_{i=1}^{N_\omega} \frac{1}{\lambda_\omega(t_i^\omega)}. \quad (24)$$

Next, we will tackle the second part:

$$- \int_0^T \lambda_\omega(t) dt. \quad (25)$$

We note that the above term involves the integral of  $\lambda_\omega(t)$  which is a function of  $\mu_\omega$ . Taking the partial derivative with respect to  $\mu_\omega$ , we get:

$$\frac{\partial}{\partial \mu_\omega} \left( - \int_0^T \lambda_\omega(t) dt \right) = - \int_0^T \frac{\partial \lambda_\omega(t)}{\partial \mu_\omega} dt. \quad (26)$$

By the simple calculation,  $\frac{\partial \lambda_\omega(t)}{\partial \mu_\omega} = 1$ , we arrive at:

$$-\int_0^T 1 dt = -T. \quad (27)$$

Combining the two parts, we obtain the gradient:

$$\frac{\partial \mathcal{L}}{\partial \mu_\omega} = \sum_{i=1}^{N_\omega} \frac{1}{\lambda_\omega(t_i^\omega)} - T. \quad (28)$$

Thus, the gradient of the log-likelihood function  $\mathcal{L}$  with respect to  $\mu_\omega$  is given by:

$$\frac{\partial \mathcal{L}}{\partial \mu_\omega} = \sum_{i=1}^{N_\omega} \frac{1}{\lambda_\omega(t_i^\omega)} - T, \quad (29)$$

which can be interpreted as follows: the first term  $\sum_{i=1}^{N_\omega} \frac{1}{\lambda_\omega(t_i^\omega)}$  is the gradient based on the actual events, reflecting the relationship between the observed event times and the intensity function; the second term  $-T$  is the penalty term, which reflects the contribution of the expected number of events over the entire time window, ensuring that the model does not predict excessively high event frequencies during periods without events.

### 9.3 B

The log-likelihood function for the high-dimensional Hawkes process involves two main terms: the log term and the integral term. The log-likelihood function for the parameter  $\alpha_{\omega, \omega'}$  is given by:

$$\mathcal{L} = \sum_{i=1}^{N_\omega} \ln(\lambda_\omega(t_i^\omega)) - \int_0^T \lambda_\omega(t) dt, \quad (30)$$

where  $\lambda_\omega(t)$  is the intensity function for the process.

#### Step 1: Log Term Gradient

Recall that the log term is defined as:

$$\sum_{i=1}^{N_\omega} \ln(\lambda_\omega(t_i^\omega)). \quad (31)$$

Taking the derivative with respect to  $\alpha_{\omega, \omega'}$ , we deduce that:

$$\frac{\partial}{\partial \alpha_{\omega, \omega'}} \ln(\lambda_\omega(t_i^\omega)) = \frac{1}{\lambda_\omega(t_i^\omega)} \cdot \frac{\partial \lambda_\omega(t_i^\omega)}{\partial \alpha_{\omega, \omega'}}. \quad (32)$$

We then substitute the intensity function into the above equation:

$$\lambda_\omega(t) = \mu_\omega + \sum_{\omega' \in \Omega} \sum_{t_j^{\omega'} \leq t} \alpha_{\omega, \omega'} \phi_{\omega, \omega'}(t - t_j^{\omega'}), \quad (33)$$

and calculate the derivative of  $\lambda_\omega(t)$  with respect to  $\alpha_{\omega, \omega'}$  as:

$$\frac{\partial \lambda_\omega(t)}{\partial \alpha_{\omega, \omega'}} = \sum_{t_j^{\omega'} \leq t} \phi_{\omega, \omega'}(t - t_j^{\omega'}). \quad (34)$$

Thus, the gradient of the log term is:

$$\frac{\partial}{\partial \alpha_{\omega, \omega'}} \ln(\lambda_\omega(t_i^\omega)) = \frac{1}{\lambda_\omega(t_i^\omega)} \cdot \sum_{j=1}^{N_{\omega'}} e^{-\beta_{\omega, \omega'}(t_i^\omega - t_j^{\omega'})} \mathbf{1}_{\{t_j^{\omega'} < t_i^\omega\}}. \quad (35)$$

The full gradient for the log term is:

$$\sum_{i=1}^{N_\omega} \frac{1}{\lambda_\omega(t_i^\omega)} \sum_{j=1}^{N_{\omega'}} e^{-\beta_{\omega, \omega'}(t_i^\omega - t_j^{\omega'})} \mathbf{1}_{\{t_j^{\omega'} < t_i^\omega\}}. \quad (36)$$

#### Step 2: Integral Term Gradient

Recall that the integral term is given by:

$$-\int_0^T \lambda_\omega(t) dt. \quad (37)$$

The derivative with respect to  $\alpha_{\omega, \omega'}$  is:

$$\frac{\partial}{\partial \alpha_{\omega, \omega'}} \left( -\int_0^T \lambda_\omega(t) dt \right) = -\int_0^T \frac{\partial \lambda_\omega(t)}{\partial \alpha_{\omega, \omega'}} dt. \quad (38)$$

We calculate the derivative of  $\lambda_\omega(t)$  with respect to  $\alpha_{\omega, \omega'}$  and get:

$$\frac{\partial \lambda_\omega(t)}{\partial \alpha_{\omega, \omega'}} = \sum_{t_j^{\omega'} \leq t} e^{-\beta_{\omega, \omega'}(t - t_j^{\omega'})} \mathbf{1}_{\{t \geq t_j^{\omega'}\}}. \quad (39)$$

Therefore, the gradient of the integral term can be written as:

$$-\int_0^T \sum_{t_j^{\omega'} \leq t} e^{-\beta_{\omega, \omega'}(t - t_j^{\omega'})} \mathbf{1}_{\{t \geq t_j^{\omega'}\}} dt. \quad (40)$$

We then replace the indicator function and perform the integral from  $t_j^{\omega'}$  to  $T$ :

$$\int_{t_j^{\omega'}}^T e^{-\beta_{\omega,\omega'}(t-t_j^{\omega'})} dt = \frac{1}{\beta_{\omega,\omega'}} \left(1 - e^{-\beta_{\omega,\omega'}(T-t_j^{\omega'})}\right). \quad (41)$$

Thus, the gradient of the integral term is calculated as:

$$-\sum_{j=1}^{N_{\omega'}} \frac{1}{\beta_{\omega,\omega'}} \left[1 - e^{-\beta_{\omega,\omega'}(T-t_j^{\omega'})}\right]. \quad (42)$$

### Step 3: Final Gradient Expression

Combining the log term and integral term gradients, we obtain the complete gradient with respect to  $\alpha_{\omega,\omega'}$  as:

$$\frac{\partial \mathcal{L}}{\partial \alpha_{\omega,\omega'}} = \sum_{i=1}^{N_{\omega}} \frac{1}{\lambda_{\omega}(t_i^{\omega})} \sum_{j=1}^{N_{\omega'}} e^{-\beta_{\omega,\omega'}(t_i^{\omega}-t_j^{\omega'})} \mathbf{1}_{\{t_j^{\omega'} < t_i^{\omega}\}} - \quad (43)$$

$$\sum_{j=1}^{N_{\omega'}} \frac{1}{\beta_{\omega,\omega'}} \left[1 - e^{-\beta_{\omega,\omega'}(T-t_j^{\omega'})}\right]. \quad (44)$$

## 9.4 C

The log-likelihood function for the high-dimensional Hawkes process involves two main terms: the log term and the integral term. The log-likelihood function for the parameter  $\alpha_{\omega,\omega'}$  is given by:

$$\mathcal{L} = \sum_{i=1}^{N_{\omega}} \ln(\lambda_{\omega}(t_i^{\omega})) - \int_0^T \lambda_{\omega}(t) dt, \quad (45)$$

where  $\lambda_{\omega}(t)$  is the intensity function for the process.

### Step 1: Log Term Gradient

The log term is:

$$\sum_{i=1}^{N_{\omega}} \ln(\lambda_{\omega}(t_i^{\omega})). \quad (46)$$

Taking the derivative with respect to  $\alpha_{\omega,\omega'}$ :

$$\frac{\partial}{\partial \alpha_{\omega,\omega'}} \ln(\lambda_{\omega}(t_i^{\omega})) = \frac{1}{\lambda_{\omega}(t_i^{\omega})} \cdot \frac{\partial \lambda_{\omega}(t_i^{\omega})}{\partial \alpha_{\omega,\omega'}}. \quad (47)$$

Using the intensity function:

$$\lambda_{\omega}(t) = \mu_{\omega} + \sum_{\omega' \in \Omega} \sum_{t_j^{\omega'} \leq t} \alpha_{\omega,\omega'} \phi_{\omega,\omega'}(t - t_j^{\omega'}). \quad (48)$$

The derivative of  $\lambda_{\omega}(t)$  with respect to  $\alpha_{\omega,\omega'}$  is:

$$\frac{\partial \lambda_{\omega}(t)}{\partial \alpha_{\omega,\omega'}} = \sum_{t_j^{\omega'} \leq t} \phi_{\omega,\omega'}(t - t_j^{\omega'}). \quad (49)$$

Thus, the gradient of the log term is:

$$\frac{\partial}{\partial \alpha_{\omega,\omega'}} \ln(\lambda_{\omega}(t_i^{\omega})) = \frac{1}{\lambda_{\omega}(t_i^{\omega})} \cdot \sum_{j=1}^{N_{\omega'}} e^{-\beta_{\omega,\omega'}(t_i^{\omega}-t_j^{\omega'})} \mathbf{1}_{\{t_j^{\omega'} < t_i^{\omega}\}}. \quad (50)$$

The full gradient for the log term is:

$$\sum_{i=1}^{N_{\omega}} \frac{1}{\lambda_{\omega}(t_i^{\omega})} \sum_{j=1}^{N_{\omega'}} e^{-\beta_{\omega,\omega'}(t_i^{\omega}-t_j^{\omega'})} \mathbf{1}_{\{t_j^{\omega'} < t_i^{\omega}\}}. \quad (51)$$

### Step 2: Integral Term Gradient

The integral term is:

$$-\int_0^T \lambda_{\omega}(t) dt. \quad (52)$$

The derivative with respect to  $\alpha_{\omega,\omega'}$  is:

$$\frac{\partial}{\partial \alpha_{\omega,\omega'}} \left(-\int_0^T \lambda_{\omega}(t) dt\right) = -\int_0^T \frac{\partial \lambda_{\omega}(t)}{\partial \alpha_{\omega,\omega'}} dt. \quad (53)$$

We know that:

$$\frac{\partial \lambda_{\omega}(t)}{\partial \alpha_{\omega,\omega'}} = \sum_{t_j^{\omega'} \leq t} e^{-\beta_{\omega,\omega'}(t-t_j^{\omega'})} \mathbf{1}_{\{t \geq t_j^{\omega'}\}}. \quad (54)$$

Therefore, the gradient of the integral term is:

$$-\int_0^T \sum_{t_j^{\omega'} \leq t} e^{-\beta_{\omega,\omega'}(t-t_j^{\omega'})} \mathbf{1}_{\{t \geq t_j^{\omega'}\}} dt. \quad (55)$$

We perform the integral from  $t_j^{\omega'}$  to  $T$ :

$$\int_{t_j^{\omega'}}^T e^{-\beta_{\omega,\omega'}(t-t_j^{\omega'})} dt = \frac{1}{\beta_{\omega,\omega'}} \left(1 - e^{-\beta_{\omega,\omega'}(T-t_j^{\omega'})}\right). \quad (56)$$

Thus, the gradient of the integral term is:

$$-\sum_{j=1}^{N_{\omega'}} \frac{1}{\beta_{\omega, \omega'}} \left[ 1 - e^{-\beta_{\omega, \omega'}(T-t_j^{\omega'})} \right]. \quad (57)$$

### Final Gradient Expression

Combining the log term and integral term gradients, the complete gradient with respect to  $\alpha_{\omega, \omega'}$  is:

$$\frac{\partial \mathcal{L}}{\partial \alpha_{\omega, \omega'}} = \sum_{i=1}^{N_{\omega}} \frac{1}{\lambda_{\omega}(t_i^{\omega})} \sum_{j=1}^{N_{\omega'}} e^{-\beta_{\omega, \omega'}(t_i^{\omega} - t_j^{\omega'})} \mathbf{1}_{\{t_j^{\omega'} < t_i^{\omega}\}} - \quad (58)$$

$$\sum_{j=1}^{N_{\omega'}} \frac{1}{\beta_{\omega, \omega'}} \left[ 1 - e^{-\beta_{\omega, \omega'}(T-t_j^{\omega'})} \right]. \quad (59)$$